OPTICS

A gain route to reversed Cherenkov radiation

Ruoxi Chen[1,2], Zheng Gong[1,2], Zun Wang[3], Xiangfeng Xi[1,2], Bowen Zhang[1,2], Yi Yang[4,5], Baile Zhang[6,7], Ido Kaminer[8]*, Hongsheng Chen[1,2,9,10]*, Xiao Lin[1,2]*

In his landmark paper from 1968, Veselago showed that Cherenkov radiation can be reversed in materials with a negative index of refraction, inspiring substantial research into such materials in what became one of the cornerstone concepts of the field of metamaterials. Following and ongoing investigations of reversed Cherenkov radiation considered it impossible to occur from a homogeneous isotropic slab with a positive refractive index. Here, we break this long-held belief by finding the emergence of reversed Cherenkov radiation from a positive-index isotropic slab by exploiting optical gain. We find precise conditions under which the backward-propagating Cherenkov radiation is maintained while the forward-propagating one is suppressed. Counterintuitively, the intensity and the angular spread of reversed Cherenkov radiation can be made robust to the slab thickness. Under this scenario, increasing the optical gain could decrease the intensity and increase the radiation angular spread.

INTRODUCTION

When a charged particle moves with a velocity larger than the phase velocity of light in a surrounding material, that particle emits light into a highly directional cone. This exotic light emission process, known as Cherenkov radiation, was experimentally observed by Cherenkov (*1*) under the guidance of Vavilov and later theoretically explained by Tamm and Frank (*2*). The many variants of Cherenkov radiation phenomena (*3*–*8*) are now a common sight in modern physics (e.g., the bluish glow of an underwater nuclear reactor). According to the famous Frank-Tamm formula $\cos\theta = \frac{c}{nv}$, the angle θ of light emission (also known as the Cherenkov angle) is related in a unique way to the particle velocity $v = |\overline{v}|$, where n is the refractive index of the surrounding material and c is the speed of light in vacuum. Enabled by this unique feature, the Cherenkov radiation is crucial to many practical applications, ranging from particle detectors/counters (*9*–*12*) and light sources (*13*–*17*) to biomedical imaging (*18*–*20*) and photodynamic therapy (*21*–*23*).

Upon close inspection of the Frank-Tamm formula, the Cherenkov angle inside the conventional material with $n > 0$ has $\theta < 90°$. That is, conventional Cherenkov radiation in positive-index materials is emitted in the forward direction relative to the direction of the particle motion. The forward direction is often undesirable. For example, Cherenkov detectors that rely on measuring Cherenkov radiation must cope with the energetic charged particles that cause radiation damage. This radiation damage limits the performance of particle identification and counting (*24*–*26*). Radiation emission in the backward direction is desired for both practical applications that rely on the Cherenkov effect (e.g., the development of advanced Cherenkov detectors with improved performance) and for fundamental reasons that relate to the nature of radiation emission in optical materials.

The most famous way to create such unconventional Cherenkov radiation is using exotic materials with $n < 0$ (*27*–*33*), for which $\theta > 90°$ in the Frank-Tamm formula. In this case, the emitted photons and the emitting charged particles are spatially well separated in opposite directions. This unconventional phenomenon, as first proposed by Veselago (*34*) in 1968, is the so-called reversed Cherenkov radiation (*35*–*38*). This effect is a milestone today in the investigation of unusual phenomena associated with negative-index materials [e.g., negative refraction (*27*–*33*) and inverse Doppler effect (*39*–*44*)]. Soon after the successful fabrication of negative-index materials in 2001 (*33*), reversed Cherenkov radiation from negative-index materials has also been successfully observed in recent experiments (*25*, *26*, *45*–*47*). In addition to negative-index materials, people later found that reversed Cherenkov radiation could also occur in anisotropic materials (e.g., hyperbolic materials) (*48*–*51*) and photonic crystals (*52*–*55*). Essentially, the occurrence of reversed Cherenkov radiation requires the surrounding material—such as negative-index materials, hyperbolic materials, and photonic crystals—to support a judiciously designed photonic eigenmode, whose group velocity $\overline{v}_g$ has the antiparallel component with respect to the particle velocity $\overline{v}$, namely, $\overline{v} \cdot \overline{v}_g < 0$. In contrast, conventional Cherenkov radiation inside any isotropic positive-index material has $\overline{v} \cdot \overline{v}_g > 0$. Whether reversed Cherenkov radiation can emerge for $\overline{v} \cdot \overline{v}_g > 0$ remains elusive.

Here, we reveal a mechanism for creating the effective reversed Cherenkov radiation from a positive-index isotropic slab by exploiting the optical gain. This finding breaks the long-standing belief that the reversed Cherenkov radiation occurs only under the scenario of $\overline{v} \cdot \overline{v}_g < 0$. We show that a judiciously designed gain medium can not only maintain backward-propagating radiation emission but also even suppress the forward-propagating emission. This way, while the initially induced Cherenkov radiation inside the gain material still has $\overline{v} \cdot \overline{v}_g > 0$, the modified Cherenkov radiation after the interaction with the gain slab could transmit only into the backward

[1]Interdisciplinary Center for Quantum Information, State Key Laboratory of Extreme Photonics and Instrumentation, Zhejiang Key Laboratory of Intelligent Electromagnetic Control and Advanced Electronic Integration, College of Information Science & Electronic Engineering, Zhejiang University, Hangzhou 310027, China. [2]International Joint Innovation Center, The Electromagnetics Academy at Zhejiang University, Zhejiang University, Haining 314400, China. [3]Chu Kochen Honors College, Zhejiang University, Hangzhou 310027, China. [4]Department of Physics, University of Hong Kong, Hong Kong 999077, China. [5]HK Institute of Quantum Science and Technology, University of Hong Kong, Hong Kong 999077, China. [6]Division of Physics and Applied Physics, School of Physical and Mathematical Sciences, Nanyang Technological University, Singapore 637371, Singapore. [7]Centre for Disruptive Photonic Technologies, Nanyang Technological University, Singapore 637371, Singapore. [8]Department of Electrical and Computer Engineering, Technion-Israel Institute of Technology, Haifa 32000, Israel. [9]Key Laboratory of Advanced Micro/Nano Electronic Devices & Smart Systems of Zhejiang, Jinhua Institute of Zhejiang University, Zhejiang University, Jinhua 321099, China. [10]Shaoxing Institute of Zhejiang University, Zhejiang University, Shaoxing 312000, China.
*Corresponding author. Email: kaminer@technion.ac.il (I.K.); hansomchen@zju.edu.cn (H.C.); xiaolinzju@zju.edu.cn (X.L.)

vacuum region, leading to effective reversed Cherenkov radiation. We highlight that the connection between the reversed Cherenkov radiation and the optical gain has never been explored before, despite the long research history of free-electron radiation (*56*–*70*) and optical gain (*71*–*83*). Meanwhile, whereas the pseudo-Brewster effect of gain materials was recently reported possible to simultaneously enhance the radiation intensity and directionality of transition radiation (*84*) (another typical type of free-electron radiation that occurs when an electron moves across an optical interface) (*85*–*95*), the influence of optical gain on the performance of Cherenkov radiation remains underexplored (*96*).

RESULTS

We begin with the conceptual demonstration of reversed Cherenkov radiation from a gain slab in Fig. 1. In practice, the optical gain could be obtained, for example, by optically pumped dye molecules at the visible regime (*71*–*73*), solid-state gain media at the infrared regime (*74*, *75*), and negative-resistance components at the microwave regime (*76*–*79*). Without loss of generality, the swift electron propagates with a velocity of $\bar{v} = \hat{z}v$ and perpendicularly penetrates through a dielectric slab. To avoid the potential inelastic electron scattering, which may change the property of swift electron itself and induce other types of free-electron radiation (e.g., bremsstrahlung radiation), a tiny hole with its center along the trajectory of electron could be drilled for the designed slab (*97*, *98*). This slab has a thickness of d and is denoted as region 2 with a relative permittivity $\varepsilon_{r,2}$ and a relative permeability $\mu_{r,2}$. For illustration, $v/c = 0.6$ and $d/\lambda_0 = 100$ are chosen in Fig. 1, where λ_0 (e.g., $\lambda_0 = 30$ μm in this work) is the wavelength in vacuum. The dielectric slab has a positive refractive index and optical gain, such that $\varepsilon_{r,2} = 3 - 0.1i$ and $\mu_{r,2} = 1$ are adopted in Fig. 1 (A and B). According to the phase matching condition, the Cherenkov angles in the vacuum region (i.e., region 1 or 3 in Fig. 1A) should be $\theta_{CR} = 28.6°$. As expected, there is the emergence of a backward radiation peak at the prescribed Cherenkov angle θ_{CR}, which corresponds to the signal of backward Cherenkov radiation into the vacuum. By contrast, the intensity of forward radiation in Fig. 1B is two orders of magnitude weaker than that of backward radiation. Moreover, there is no forward radiation peak at θ_{CR}. This indicates the disappearance of forward Cherenkov radiation into the vacuum. In short, the effective reversed Cherenkov radiation from a gain slab in Fig. 1 (A and B) is featured with the disappearance of forward Cherenkov radiation. This feature of reversed Cherenkov radiation from a gain slab markedly differs from that of a negative-index slab. For comparison, when the dielectric slab has a negative index, $\varepsilon_{r,2} = -3$ and $\mu_{r,2} = -1$ are used in Fig. 1 (C and D). From Fig. 1D, the signal of forward Cherenkov radiation would show up simultaneously with the signal of backward Cherenkov radiation at the prescribed Cherenkov angle θ_{CR}. Essentially, the forward Cherenkov radiation in Fig. 1 (C and D) comes from the reflection of backward Cherenkov radiation due to the nonzero reflection at the interface between the vacuum and the negative-index medium.

We now proceed to explore the underlying reason for the disappearance of forward Cherenkov radiation from a gain slab. By following Ginzburg and Frank's theory of free-electron radiation (*84*–*90*), the angular spectral energy densities for the backward radiation $U_B(\theta_B)$ and the forward radiation $U_F(\theta_F)$ can be expressed as

$$U_B(\theta_B) = \frac{q^2 \cos^2\theta_B}{4\pi^3 \varepsilon_0^2 c \sin^2\theta_B} |A_B|^2 \quad (1)$$

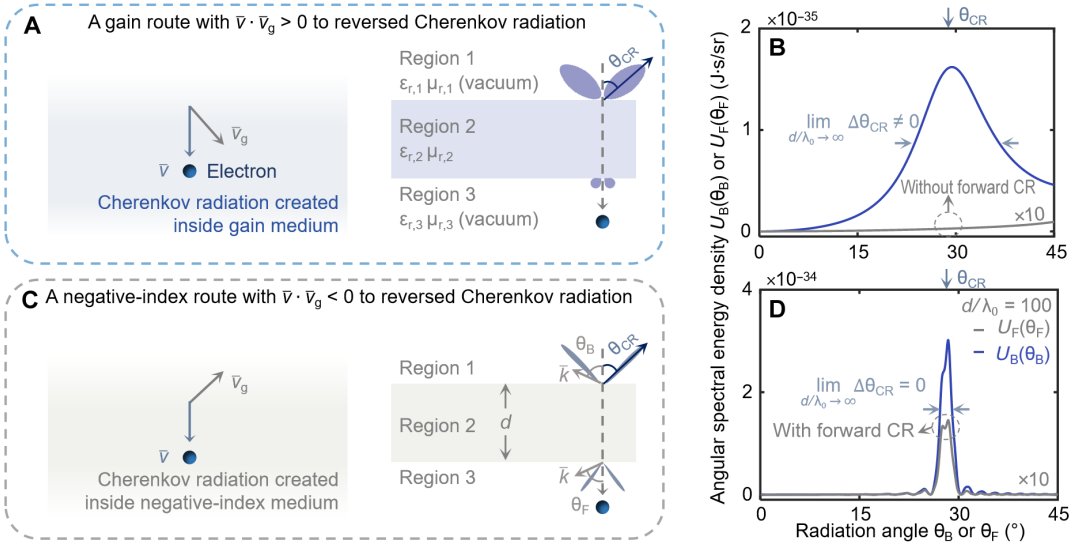

Fig. 1. Conceptual demonstration of a gain route to reversed Cherenkov radiation. A moving electron with a velocity $\bar{v} = \hat{z}v$ perpendicularly penetrates through a slab with a thickness d, a relative permittivity $\varepsilon_{r,2}$, and a relative permeability $\mu_{r,2}$. (**A** and **B**) A gain route with $\bar{v} \cdot \bar{v}_g > 0$ to reversed Cherenkov radiation: The slab is composed of a gain medium with $\bar{v} \cdot \bar{v}_g > 0$, where $\bar{v}_g$ is the group velocity of excited eigenmodes in the corresponding medium. The Cherenkov radiation is first created inside the gain medium and later is transmitted into the vacuum region. (**C** and **D**) A negative-index route with $\bar{v} \cdot \bar{v}_g < 0$ to reversed Cherenkov radiation by Veselago: The slab is composed of a negative-index medium with $\bar{v} \cdot \bar{v}_g < 0$. Without further specification, here and below, we set $\varepsilon_{r,2} = 3 - 0.1i$ and $\mu_{r,2} = 1$ for the gain medium, $\varepsilon_{r,2} = -3$ and $\mu_{r,2} = -1$ for the negative-index medium, the working wavelength $\lambda_0 = 30$ μm, $d/\lambda_0 = 100$, $v/c = 0.6$, and both regions 1 and 3 being vacuum, where c is the light speed in vacuum. $U_B(\theta_B)$ [$U_F(\theta_F)$] is the angular spectral energy density of the backward radiation into region 1 (the forward radiation into region 3), where the radiation angle θ_B in region 1 (θ_F in region 3) is the angle between the wave vector $\bar{k}$ of emitted light and $-\bar{v}$ ($+\bar{v}$). The angular spreading factor $\Delta\theta_{CR}$ corresponds to the full width at half maximum of the backward Cherenkov radiation into region 1.

$$U_F(\theta_F) = \frac{q^2\cos^2\theta_F}{4\pi^3\varepsilon_0^2 c\sin^2\theta_F}|A_F|^2 \quad (2)$$

where θ_B (θ_F) is the angle between the wave vector of emitted light in vacuum and $-\overline{v}$ ($+\overline{v}$) in Fig. 1A, ε_0 is the permittivity in vacuum, and q is the electron charge. After some algebra, the radiation coefficients A_B and A_F in Eqs. 1 and 2 can be obtained as

$$A_B = a_{1,2}^{0,B} + a_{1,2}^{0,F}\frac{R_{2,3}T_{2,1}}{1-R_{2,1}R_{2,3}e^{2ik_{z,2}d}}e^{2ik_{z,2}d} + a_{2,3}^{0,B}\frac{T_{2,1}}{1-R_{2,1}R_{2,3}e^{2ik_{z,2}d}}e^{i\frac{\omega}{v}d}e^{ik_{z,2}d} \quad (3)$$

$$A_F = a_{2,3}^{0,F}e^{i\frac{\omega}{v}d} + a_{1,2}^{0,F}\frac{T_{2,3}}{1-R_{2,1}R_{2,3}e^{2ik_{z,2}d}}e^{ik_{z,2}d} + a_{2,3}^{0,B}\frac{R_{2,1}T_{2,3}}{1-R_{2,1}R_{2,3}e^{2ik_{z,2}d}}e^{i\frac{\omega}{v}d}e^{2ik_{z,2}d} \quad (4)$$

where $a_{j,j+1}^{0,B} = \frac{\frac{v}{c}\cdot\frac{k_\perp^2c^2}{\omega^2}}{\varepsilon_{r,j}\frac{k_{z,j+1}}{\omega/c}+\varepsilon_{r,j+1}\frac{k_{z,j}}{\omega/c}}\left[\frac{\frac{\varepsilon_{r,j+1}}{\varepsilon_{r,j}}-\frac{k_{z,j+1}}{\omega/v}}{\left(1+\frac{k_{z,j}}{\omega/v}\right)\left(1-\frac{k_{z,j}}{\omega/v}\right)}-\frac{1}{1+\frac{k_{z,j+1}}{\omega/v}}\right]$ and $a_{j,j+1}^{0,F} = \frac{\frac{v}{c}\cdot\frac{k_\perp^2c^2}{\omega^2}}{\varepsilon_{r,j}\frac{k_{z,j+1}}{\omega/c}+\varepsilon_{r,j+1}\frac{k_{z,j}}{\omega/c}}\left[\frac{1}{1-\frac{k_{z,j}}{\omega/v}}-\frac{\frac{\varepsilon_{r,j}}{\varepsilon_{r,j+1}}+\frac{k_{z,j}}{\omega/v}}{\left(1+\frac{k_{z,j+1}}{\omega/v}\right)\left(1-\frac{k_{z,j+1}}{\omega/v}\right)}\right]$ are the coefficients related to the backward and forward radiation from a single interface between region j and $j+1$; $\overline{k}_j = \overline{k}_\perp + \hat{z}k_{z,j}$ is the wave vector of light in region j ($j = 1$ or 2), $k_{z,j} = \sqrt{\frac{\omega^2}{c^2}\mu_{r,j}\varepsilon_{r,j} - k_\perp^2}$, $\overline{k}_\perp = \hat{x}k_x + \hat{y}k_y$, and $k_\perp = |\overline{k}_\perp|$; $R_{j,j+1}$, $R_{j+1,j}$, $T_{j,j+1}$, and $T_{j+1,j}$ are related to the reflection and transmission coefficients at the interface between region j and $j+1$, respectively. Because $\mathrm{Im}(k_{z,2}) < 0$ for the gain slab in Fig. 1A, we have $|e^{2ik_{z,2}d}| \to \infty$ and $|R_{2,1}R_{2,3}e^{2ik_{z,2}d}| \gg 1$ if $d/\lambda_0 \gg 1$. Accordingly, we have $\lim_{d/\lambda_0\gg1}\frac{e^{ik_{z,2}d}}{1-R_{2,1}R_{2,3}e^{2ik_{z,2}d}} = 0$ and $\lim_{d/\lambda_0\gg1}\frac{e^{2ik_{z,2}d}}{1-R_{2,1}R_{2,3}e^{2ik_{z,2}d}} = \frac{-1}{R_{2,1}R_{2,3}}$ in Eqs. 3 and 4. On the basis of this knowledge, the radiation coefficients A_B and A_F in Eqs. 3 and 4 can be further simplified to

$$\lim_{d/\lambda_0\gg1}A_B \propto \left[\frac{1}{\left(1-\frac{k_{z,2}}{\omega/v}\right)}\cdot m_0 + m_1\right] \quad (5)$$

$$\lim_{d/\lambda_0\gg1}A_F \propto \left[\frac{1}{\left(1-\frac{k_{z,2}}{\omega/v}\right)}\cdot 0 + m_2\right] \quad (6)$$

where $m_0 = \frac{\left(\frac{\varepsilon_{r,1}}{\varepsilon_{r,2}}+\frac{k_{z,1}}{\omega/v}\right)\frac{\varepsilon_{r,2}k_{z,2}}{\varepsilon_{r,1}k_{z,2}-\varepsilon_{r,2}k_{z,1}}-\left(1+\frac{k_{z,2}}{\omega/v}\right)}{\left(1+\frac{k_{z,2}}{\omega/v}\right)}$, $m_1 = \frac{\left(\frac{\varepsilon_{r,2}}{\varepsilon_{r,1}}-\frac{k_{z,2}}{\omega/v}\right)-\frac{\varepsilon_{r,2}k_{z,2}}{\varepsilon_{r,1}k_{z,2}-\varepsilon_{r,2}k_{z,1}}\left(1+\frac{k_{z,1}}{\omega/v}\right)}{\left(1+\frac{k_{z,1}}{\omega/v}\right)\left(1-\frac{k_{z,1}}{\omega/v}\right)}$, and $m_2 = -\left[\frac{\varepsilon_{r,3}k_{z,2}+\varepsilon_{r,2}k_{z,3}}{\left(1+\frac{k_{z,2}}{\omega/v}\right)\left(\varepsilon_{r,3}k_{z,2}-\varepsilon_{r,2}k_{z,3}\right)}+\frac{\left(\frac{\varepsilon_{r,2}}{\varepsilon_{r,3}}+\frac{k_{z,2}}{\omega/v}\right)-\frac{\varepsilon_{r,2}k_{z,2}}{\varepsilon_{r,3}k_{z,2}-\varepsilon_{r,2}k_{z,3}}\left(1-\frac{k_{z,3}}{\omega/v}\right)}{\left(1+\frac{k_{z,3}}{\omega/v}\right)\left(1-\frac{k_{z,3}}{\omega/v}\right)}\right]$. Note that all coefficients of m_0, m_1, and m_2 in Eqs. 5 and 6 are irrelevant to the term of $\frac{1}{1-\frac{k_{z,2}}{\omega/v}}$.

Upon close inspection of Eq. 5, there would be a pole if $\left(1-\frac{k_{z,2}}{\omega/v}\right)=0$, namely, $k_{z,2} = \omega/v$ and $k_\perp = \sqrt{\frac{\omega^2}{c^2}\varepsilon_{r,2}\mu_{r,2} - k_{z,2}^2} = \sqrt{\frac{\omega^2}{c^2}\varepsilon_{r,2}\mu_{r,2} - \frac{\omega^2}{v^2}} = k_{\perp,CR}$. Essentially, this pole corresponds to the Cherenkov radiation inside the gain medium and is then termed as the Cherenkov pole below. Because $\mathrm{Im}(\varepsilon_{r,2}) < 0$ for gain medium, this Cherenkov pole appears in the fourth quadrant of the complex $k_\perp$ plane, namely, $\mathrm{Re}(k_{\perp,CR}) > 0$ and $\mathrm{Im}(k_{\perp,CR}) < 0$. When considering Eq. 5 on the real axis of $k_\perp$, the value of $|A_B|$ becomes finite and would have a maximum at $k_\perp = \mathrm{Re}(k_{\perp,CR})$. Because $k_0\sin\theta_B = \mathrm{Re}(k_\perp)$ in the vacuum region according to the phase-matching condition, we further have $\sin\theta_{CR} = \mathrm{Re}(k_{\perp,CR})/k_0$ for the Cherenkov radiation propagating into the backward vacuum region, where $k_0 = \omega/c$. By substituting Eq. 5 into Eq. 1, correspondingly, the backward angular spectral energy density $U_B(\theta_B)$ would have a radiation peak at $\theta_B = \theta_{CR}$. In short, the Cherenkov pole of $|A_B|$ in the complex $k_\perp$ plane is the fundamental reason for the emergence of backward radiation peak from a gain slab at $\theta_B = \theta_{CR}$ in Fig. 1A.

By contrast, because the factor related to the term of $\frac{1}{\left(1-\frac{k_{z,2}}{\omega/v}\right)}$ is zero in Eq. 6, there would be no Cherenkov pole for A_F. Accordingly, $|A_F|$ does not necessarily have a maximum at $k_\perp = \mathrm{Re}(k_{\perp,CR})$. By substituting Eq. 6 into Eq. 2, the forward angular spectral energy density $U_F(\theta_F)$ also does not have a radiation peak at $\theta_F = \theta_{CR}$. In other words, the disappearance of the forward radiation peak from a gain slab at $\theta_F = \theta_{CR}$ in Fig. 1A is essentially attributed to the disappearance of Cherenkov pole of $|A_F|$ in the complex $k_\perp$ plane. This fact is further verified in Fig. 2. To be specific, Fig. 2 (A and B) shows that the disappearance of forward Cherenkov radiation from a gain slab would always occur when the slab thickness is sufficiently large (i.e., $d/\lambda_0 \gg 1$), and it is also irrelevant to the electron velocity. By contrast, we further show in Fig. 2 (C and D) that there would be no suppression of the forward Cherenkov radiation at $\theta_F = \theta_{CR}$ from a negative-index slab, as long as the backward Cherenkov radiation shows up.

In short, the reversed Cherenkov radiation is closely related to both the emergence of Cherenkov pole for A_B and the disappearance of Cherenkov pole for A_F. In other words, the emergence of reversed Cherenkov radiation is essentially the combined effect between the conventional Cherenkov radiation inside gain media and the exotic light interference from a sufficiently thick gain slab. On the other hand, we highlight that the analysis of light interference from gain slabs (e.g., the calculation of reflection and transmission coefficients) is generally no longer valid via ray optics or geometrical optics but should resort to wave optics by critically matching the electromagnetic boundary conditions. Because of the invalidation of ray optics, it might be not that straightforward to understand the revealed phenomenon of reversed Cherenkov radiation.

Because Eqs. 5 and 6 are fulfilled as long as $d/\lambda_0 \gg 1$, Eqs. 5 and 6 further indicate that the intensity of reversed Cherenkov radiation from a gain slab could be insensitive to the slab thickness in Fig. 3 (A to C). To be specific, the radiation intensity at the prescribed Cherenkov angle has $U_B(\theta_{CR})/U_{0,B}(\theta_{CR}) \in [0.95, 1.05]$ for the backward radiation as long as $d \geq d_{backward}$ (see the illustration of $d_{backward}$ in Fig. 3A), where $U_{0,B}(\theta_{CR}) = \lim_{d/\lambda_0\to\infty}U_B(\theta_{CR})$. Similarly,

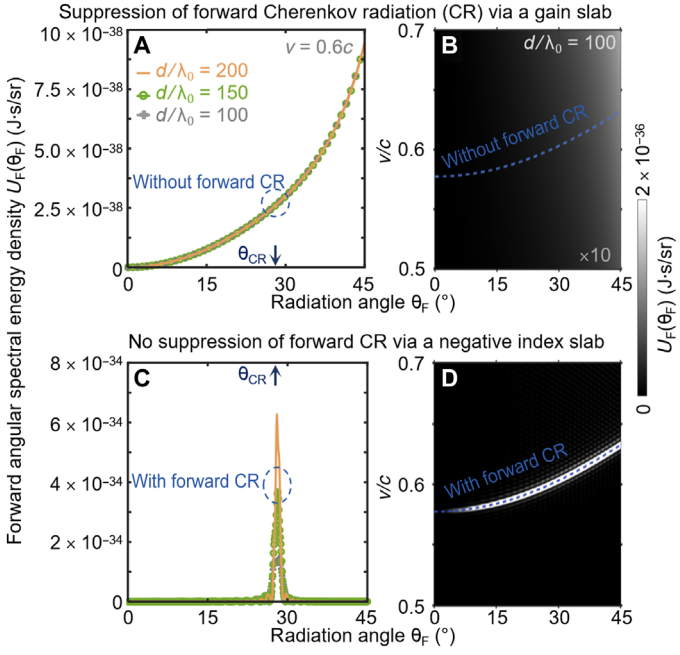

Fig. 2. Suppression of forward Cherenkov radiation via a gain slab. The structural setup here is the same as Fig. 1 except for the slab thickness d and the electron velocity v. (**A** and **C**) Influence of d on the forward angular spectral energy density $U_F(\theta_F)$ with $v/c = 0.6$. (**B** and **D**) $U_F(\theta_F)$ as a function of the radiation angle θ_F and v with $d/\lambda_0 = 100$. The blue dashed line in (B) and (D) corresponds to the relation between the Cherenkov angle θ_{CR} in vacuum and v, namely, $\theta_{CR}(v) = \arcsin\sqrt{\varepsilon_{r,2} - \frac{c^2}{v^2}}$. There is always a radiation peak at $\theta_F = \theta_{CR}$ for the case of a negative-index slab in (C) and (D), which corresponds to the existence of forward Cherenkov radiation. By contrast, there is no emergence of a radiation peak at $\theta_F = \theta_{CR}$ for the case of a gain slab in (A) and (B), which indicates the suppression of forward Cherenkov radiation.

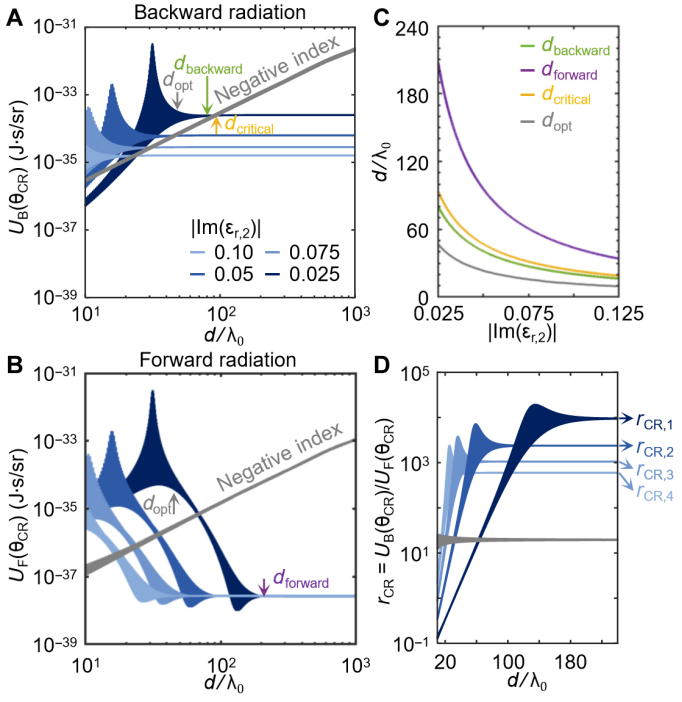

Fig. 3. Intensity of reversed Cherenkov radiation via a gain slab. (**A** and **B**) Influence of d on the angular spectral energy density of backward radiation $U_B(\theta_{CR})$ and forward radiation $U_F(\theta_{CR})$ at the Cherenkov angle under different optical gains. (**C**) Dependence of $d_{backward}$, $d_{forward}$, $d_{critical}$, and d_{opt} on $|\mathrm{Im}(\varepsilon_{r,2})|$. For various optical gains, these four parameters of $d_{backward}$, $d_{forward}$, $d_{critical}$, and d_{opt} are mathematically defined as follows: When $d \geq d_{backward}$, the backward Cherenkov radiation always has $U_B(\theta_{CR}) \in [0.95,1.05] \cdot U_{0,B}(\theta_{CR})$ in (A), where $U_{0,B}(\theta_{CR}) = \lim_{d/\lambda_0 \to \infty} U_B(\theta_{CR})$. Similarly, we have $U_F(\theta_{CR}) \in [0.95,1.05] \cdot U_{0,F}(\theta_{CR})$ as long as $d \geq d_{forward}$ in (B), where $U_{0,F}(\theta_{CR}) = \lim_{d/\lambda_0 \to \infty} U_F(\theta_{CR})$. When $d > d_{critical}$, $U_B(\theta_{CR})$ from a gain slab becomes smaller than that from a negative-index slab. When $d \geq d_{opt}$, the Cherenkov radiation always has $U_B(\theta_{CR}) \geq 4 \cdot U_F(\theta_{CR})$ in (A) and (B). (**D**) Influence of d on $r_{CR} = U_B(\theta_{CR}) / U_F(\theta_{CR})$ under different optical gains. For comparison, the reversed Cherenkov radiation via a negative-index slab is also plotted in (A), (B), and (D).

we have $U_F(\theta_{CR}) / U_{0,F}(\theta_{CR}) \in [0.95,1.05]$ for the forward radiation as long as $d \geq d_{forward}$ in Fig. 3B, where $U_{0,F}(\theta_{CR}) = \lim_{d/\lambda_0 \to \infty} U_F(\theta_{CR})$. By contrast, both intensities of backward and forward Cherenkov radiation from a negative-index slab tend to linearly increase with the slab thickness in Fig. 3 (A and B). This way, the intensity of backward Cherenkov radiation from a negative-index slab could, in principle, be larger than that from a gain slab when $d > d_{critical}$ (see the illustration of $d_{critical}$ in Fig. 3A). As summarized in Fig. 3C, we generally have $d_{forward} > d_{critical} > d_{backward}$ for various optical gains. This indicates that under optical gain, the minimum slab thickness for the full suppression of forward Cherenkov radiation in Fig. 3B is much larger than that for the saturation of backward Cherenkov radiation in Fig. 3A. In practice, to facilitate the potential observation of reversed Cherenkov radiation, the slab thickness does not need to have either $d \geq d_{forward}$ or $d \geq d_{backward}$ but only requires $d \geq d_{opt}$, so that the intensity of backward Cherenkov radiation is much larger than that of forward Cherenkov radiation, where d_{opt} is the optimal thickness of gain slabs to enable the emergence of reversed Cherenkov radiation [e.g., for illustration, here, we define that $U_B(\theta_{CR}) / U_F(\theta_{CR}) \geq 4$ is always satisfied if $d \geq d_{opt}$]. Under this scenario, we generally have $d_{opt} \ll d_{backward} < d_{forward}$ and, for example, $d_{opt}/\lambda_0 = 12$ if $|\mathrm{Im}(\varepsilon_{r,2})| = 0.1$ in Fig. 3C. We highlight that the judicious reduction of gain slab thickness is crucial to the possible observation of reversed Cherenkov radiation revealed in this work because it would not only help to largely increase the intensity of reversed Cherenkov radiation as shown in Fig. 3 (A and B) but also help to largely suppress the intensity of amplified spontaneous emission, which widely exists in active systems.

To further highlight the exotic intensity feature of reversed Cherenkov radiation from a gain slab, below, we consider the ratio $r_{CR} = U_B(\theta_{CR}) / U_F(\theta_{CR})$ between the backward and forward radiation at the prescribed Cherenkov angle in Fig. 3D. As expected, both values of r_{CR} from a gain slab and from a negative-index slab would saturate to a constant if $d/\lambda_0 \gg 1$. However, the value of r_{CR} from a gain slab could be orders of magnitude larger than that from a negative-index slab due to the possibility to fully suppress the forward Cherenkov radiation from a gain slab. On the other hand, we need to point out that despite the disappearance of forward Cherenkov radiation, the value of r_{CR} from a gain slab would not go to infinity in Fig. 3D because the intensity $U_F(\theta_{CR})$ of forward radiation at the prescribed Cherenkov angle from a gain slab is not

strictly zero in Fig. 3B. Essentially, the nonzero but relatively small value of $U_F(\theta_{CR})$ in Fig. 3B originates from the emergence of transition radiation, which occurs when the swift electron moves across the interface between vacuum and the gain medium and whose intensity is generally much weaker than that of Cherenkov radiation.

We now pay special attention to the directionality feature of reversed Cherenkov radiation from a gain slab in Fig. 4. We find that there is always a nonzero angular spread for the backward Cherenkov radiation in Fig. 4 (A and B), even when the thickness of gain slab goes to infinity. To be specific, we always have $\Delta\theta_0 = \lim_{d/\lambda_0\to\infty} \Delta\theta_{CR} \neq 0$, where $\Delta\theta_{CR}$ is the angular full width at half maximum for the backward radiation peak at the prescribed Cherenkov angle. By contrast, the value of $\Delta\theta_{CR}$ from a negative-index slab in Fig. 4A generally tends to decrease to zero when the slab thickness increases (namely, $\Delta\theta_0 = 0$ for the negative-index slab). Moreover, we find in Fig. 4C that the value of $\Delta\theta_0$ from an infinitely thick gain slab would increase with the optical gain. This exotic phenomenon is intrinsically related to the position (i.e., $k_\perp = k_{\perp,CR}$) of the Cherenkov pole of $|A_B|$ in the complex $k_\perp$ plane as governed by Eq. 5. On the one hand, because this Cherenkov pole from a gain slab shows up in the fourth quadrant of the complex $k_\perp$ plane in Fig. 4C, the value of $\Delta\theta_0$ would always be nonzero when considering the projection of $|A_B|$ in Eq. 5 on the real axis of $k_\perp$. The value of $\Delta\theta_0$ would converge to zero when the optical gain decreases down to zero. On the other hand, when the optical gain increases, the position of this Cherenkov pole in Fig. 4C would move further away from the real axis of $k_\perp$. Similarly, when considering the projection of $|A_B|$ on the real axis of $k_\perp$, a larger optical gain would give rise to a wider angular spread of backward Cherenkov radiation.

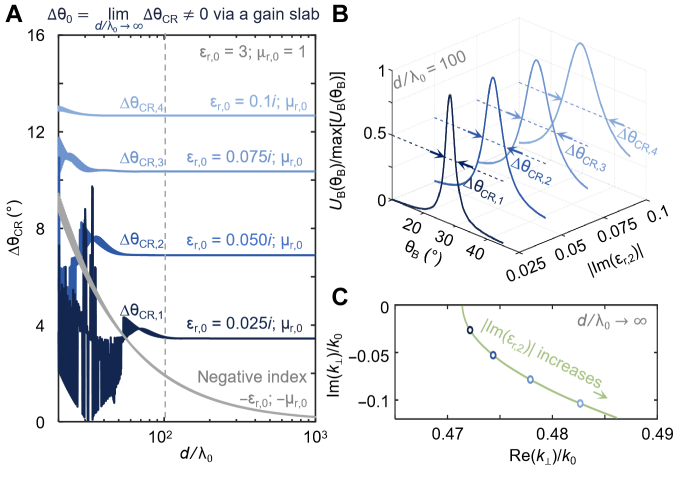

Fig. 4. Angular spread of backward Cherenkov radiation from a gain slab. (**A**) Dependence of the angular spreading factor $\Delta\theta_{CR}$ on d. We have $\lim_{d/\lambda_0\gg 1} \Delta\theta_{CR} = \Delta\theta_0 \neq 0$ for the case of a gain slab. The values for reversed Cherenkov radiation from a negative-index slab are also plotted for comparison. (**B**) Normalized backward angular spectral energy density as a function of the radiation angle θ_B for various values of the optical gain. (**C**) Influence of the optical gain on the location of poles that correspond to Cherenkov radiation in the complex $k_\perp$ plane in the limit $d/\lambda_0 \to \infty$. When the optical gain increases, the related Cherenkov pole in the fourth quadrant of the complex $k_\perp$ plane would move away from the horizontal axis of $\mathrm{Re}(k_\perp)$, which is the underlying reason for the angular spread of backward Cherenkov radiation via a gain slab.

DISCUSSION

In conclusion, we have revealed the enticing possibility of creating the reversed Cherenkov radiation from a positive-index but gain slab. Under certain circumstances, this reversed Cherenkov radiation could be accompanied with the full suppression of forward Cherenkov radiation due to the disappearance of the Cherenkov pole for the forward free-electron radiation from a gain slab. Moreover, we have found that the reversed Cherenkov radiation from a gain slab is featured with a nonzero angular spread and insensitivity to the slab thickness. These exotic features of reversed Cherenkov radiation from a gain slab might be crucial for developing many advanced Cherenkov-based applications, such as integrated light sources with enhanced intensity, miniaturized particle detectors with enhanced sensitivity, and potential biomedical applications. Meanwhile, these exotic features further indicate that there are rich physics hidden in the realm of particle-matter interactions, despite the long research history of free-electron radiation. Our work then might inspire continuous exploration of other types of free-electron radiation (e.g., Smith-Purcell radiation, transition radiation, and bremsstrahlung radiation) under the consideration of optical gain in various photonic systems (e.g., those with optical anisotropy, oriented misalignment, structural periodicity, disorders, and spatial-temporal variation).

MATERIALS AND METHODS

Derivation of free-electron radiation from an optical interface

Free-electron radiation from a single interface between region j and region $j+1$ (see the structural schematic in fig. S1) can be calculated by following Ginzburg and Frank's theory of free-electron radiation within the framework of classical electrodynamics. If the interface between region j and region $j+1$ is $z = 0$, then the backward radiation coefficient can be obtained as $a^{0,B}_{j,j+1} = \frac{\frac{v}{c}\cdot\frac{k_\perp^2 c^2}{\omega^2}}{\varepsilon_{r,j}\frac{k_{z,j+1}}{\omega/c}+\varepsilon_{r,j+1}\frac{k_{z,j}}{\omega/c}}\left[\frac{\frac{\varepsilon_{r,j+1}}{\varepsilon_{r,j}}-\frac{k_{z,j+1}}{\omega/v}}{\left(1+\frac{k_{z,j}}{\omega/v}\right)\left(1-\frac{k_{z,j}}{\omega/v}\right)}-\frac{1}{1+\frac{k_{z,j+1}}{\omega/v}}\right]$, and, similarly, the forward radiation coefficient can be expressed as $a^{0,F}_{j,j+1} = \frac{\frac{v}{c}\cdot\frac{k_\perp^2 c^2}{\omega^2}}{\varepsilon_{r,j}\frac{k_{z,j+1}}{\omega/c}+\varepsilon_{r,j+1}\frac{k_{z,j}}{\omega/c}}\left[\frac{1}{1-\frac{k_{z,j}}{\omega/v}}-\frac{\frac{\varepsilon_{r,j}}{\varepsilon_{r,j+1}}+\frac{k_{z,j}}{\omega/v}}{\left(1+\frac{k_{z,j+1}}{\omega/v}\right)\left(1-\frac{k_{z,j+1}}{\omega/v}\right)}\right]$, where $\bar{k}_j = \bar{k}_\perp + \hat{z}k_{z,j}$ is the wave vector of light in region j (= 1 or 2), $k_{z,j} = \sqrt{\frac{\omega^2}{c^2}\mu_{r,j}\varepsilon_{r,j} - k_\perp^2}$, $\bar{k}_\perp = \hat{x}k_x + \hat{y}k_y$, and $k_\perp = |\bar{k}_\perp|$. Detailed derivation is provided in section S1.

Derivation of free-electron radiation from a slab

When a fast electron perpendicularly penetrates through a slab (see the structural schematic in fig. S2), the related free-electron radiation (including Cherenkov radiation and transition radiation) can also be calculated by following Ginzburg and Frank's theory of free-electron radiation. On the basis of the result of free-electron radiation from an interface, the backward radiation coefficient A_B can be obtained as $A_B = a^{0,B}_{1,2} + a^{0,F}_{1,2}\frac{R_{2,3}T_{2,1}}{1-R_{2,1}R_{2,3}e^{2ik_{z,2}d}}e^{2ik_{z,2}d} + a^{0,B}_{2,3}\frac{T_{2,1}}{1-R_{2,1}R_{2,3}e^{2ik_{z,2}d}}e^{i\frac{\omega}{v}d}e^{ik_{z,2}d}$, and, similarly, the forward radiation coefficient A_F can be expressed as $A_F = a^{0,F}_{2,3}e^{i\frac{\omega}{v}d} + a^{0,F}_{1,2}\frac{T_{2,3}}{1-R_{2,1}R_{2,3}e^{2ik_{z,2}d}}e^{ik_{z,2}d} + a^{0,B}_{2,3}\frac{R_{2,1}T_{2,3}}{1-R_{2,1}R_{2,3}e^{2ik_{z,2}d}}e^{i\frac{\omega}{v}d}e^{2ik_{z,2}d}$, where $R_{j,j+1} = -R_{j+1,j} = \frac{\varepsilon_{r,j+1}k_{z,j}-\varepsilon_{r,j}k_{z,j+1}}{\varepsilon_{r,j+1}k_{z,j}+\varepsilon_{r,j}k_{z,j+1}}$ are the reflection coefficients, $T_{j,j+1} = \frac{2\varepsilon_{r,j}k_{z,j}}{\varepsilon_{r,j+1}k_{z,j}+\varepsilon_{r,j}k_{z,j+1}}$ and $T_{j+1,j} = \frac{2\varepsilon_{r,j+1}k_{z,j+1}}{\varepsilon_{r,j+1}k_{z,j}+\varepsilon_{r,j}k_{z,j+1}}$ are the transmission

coefficients at the interface between regions j and $j+1$ ($j=1$ or 2), respectively. Detailed derivation is provided in section S2.

Derivation of free-electron radiation from a gain slab with a sufficiently large thickness

When the slab (namely, region 2) is filled by the gain medium with a sufficiently large slab thickness (i.e., $d/\lambda_0 \gg 1$), we have $\lim_{d/\lambda_0 \gg 1} A_B = a_{1,2}^{0,B} - a_{1,2}^{0,F}\frac{T_{2,1}}{R_{2,1}} = \frac{\frac{v}{c}\cdot\frac{k_\perp^2 c^2}{\omega^2}}{\varepsilon_{r,1}\frac{k_{z,2}}{\omega/c}+\varepsilon_{r,2}\frac{k_{z,1}}{\omega/c}}\left[\frac{\left(\frac{\varepsilon_{r,1}}{\varepsilon_{r,2}}+\frac{k_{z,1}}{\omega/v}\right)\frac{\varepsilon_{r,2}k_{z,2}}{\varepsilon_{r,1}k_{z,2}-\varepsilon_{r,2}k_{z,1}}-\left(1+\frac{k_{z,2}}{\omega/v}\right)}{\left(1-\frac{k_{z,2}}{\omega/v}\right)\left(1+\frac{k_{z,2}}{\omega/v}\right)}+\right.$ $\left.\frac{\left(\frac{\varepsilon_{r,2}}{\varepsilon_{r,1}}-\frac{k_{z,2}}{\omega/v}\right)-\frac{\varepsilon_{r,2}k_{z,2}}{\varepsilon_{r,1}k_{z,2}-\varepsilon_{r,2}k_{z,1}}\left(1+\frac{k_{z,1}}{\omega/v}\right)}{\left(1+\frac{k_{z,1}}{\omega/v}\right)\left(1-\frac{k_{z,1}}{\omega/v}\right)}\right]$ and $\lim_{d/\lambda_0 \gg 1} A_F = a_{2,3}^{0,F} - a_{2,3}^{0,B}\frac{T_{2,3}}{R_{2,3}} = \frac{\frac{v}{c}\cdot\frac{k_\perp^2 c^2}{\omega^2}}{\varepsilon_{r,2}\frac{k_{z,3}}{\omega/c}+\varepsilon_{r,3}\frac{k_{z,2}}{\omega/c}}$ $\left[\frac{1}{\left(1-\frac{k_{z,2}}{\omega/v}\right)}\cdot 0-\frac{\varepsilon_{r,3}k_{z,2}+\varepsilon_{r,2}k_{z,3}}{\left(1+\frac{k_{z,2}}{\omega/v}\right)\left(\varepsilon_{r,3}k_{z,2}-\varepsilon_{r,2}k_{z,3}\right)}+\frac{\left(\frac{\varepsilon_{r,2}}{\varepsilon_{r,3}}+\frac{k_{z,2}}{\omega/v}\right)-\frac{\varepsilon_{r,2}k_{z,2}}{\varepsilon_{r,3}k_{z,2}-\varepsilon_{r,2}k_{z,3}}\left(1-\frac{k_{z,3}}{\omega/v}\right)}{\left(1+\frac{k_{z,3}}{\omega/v}\right)\left(1-\frac{k_{z,3}}{\omega/v}\right)}\right]$. After some simplification, we further have $\lim_{d/\lambda_0 \gg 1} A_B \propto \left[\frac{1}{\left(1-\frac{k_{z,2}}{\omega/v}\right)}\cdot m_0 + m_1\right]$ and $\lim_{d/\lambda_0 \gg 1} A_F \propto \left[\frac{1}{\left(1-\frac{k_{z,2}}{\omega/v}\right)}\cdot 0 + m_2\right]$, namely, Eqs. 5 and 6 in the results section. Detailed derivation is provided in section S3.

Angular spectral energy density of free-electron radiation

In section S4, the detailed calculation of backward angular spectral energy density $U_B(\theta_B)$ and forward angular spectral energy density $U_F(\theta_F)$ of free-electron radiation from either a single interface or a slab is provided. On the basis of the calculated results of the radiation field, the backward angular spectral energy density $U_B(\theta_B)$ can be obtained as $U_B(\theta_B) = \frac{\varepsilon_{r,1}\sqrt{\mu_{r,1}\varepsilon_{r,1}}q^2\cos^2\theta_B}{4\pi^3\varepsilon_0 c\sin^2\theta_B}|A_B|^2$, and similarly, the forward angular spectral energy density can be obtained as $U_F(\theta_F) = \frac{\varepsilon_{r,3}\sqrt{\mu_{r,3}\varepsilon_{r,3}}q^2\cos^2\theta_F}{4\pi^3\varepsilon_0 c\sin^2\theta_F}|A_F|^2$. Detailed derivation is provided in section S4.

Supplementary Materials

This PDF file includes:

Sections S1 to S9
Figs. S1 to S9

REFERENCES AND NOTES

1. P. A. Cherenkov, Visible emission of clean liquids by action of γ radiation. *Dokl. Akad. Nauk SSSR* **2**, 451–454 (1934).
2. I. E. Tamm, I. M. Frank, Coherent visible radiation of fast electrons in a medium. *Dokl. Akad. Nauk SSSR* **14**, 107–112 (1937).
3. Y. Adiv, H. Hu, S. Tsesses, R. Dahan, K. Wang, Y. Kurman, A. Gorlach, H. Chen, X. Lin, G. Bartal, I. Kaminer, Observation of 2D Cherenkov radiation. *Phys. Rev. X* **13**, 011002 (2023).
4. F. Liu, L. Xiao, Y. Ye, M. Wang, K. Cui, X. Feng, W. Zhang, Y. Huang, Integrated Cherenkov radiation emitter eliminating the electron velocity threshold. *Nat. Photonics* **11**, 289–292 (2017).
5. C. Roques-Carmes, S. E. Kooi, Y. Yang, N. Rivera, P. D. Keathley, J. D. Joannopoulos, S. G. Johnson, I. Kaminer, K. K. Berggren, M. Soljačić, Free-electron-light interactions in nanophotonics. *Appl. Phys. Rev.* **10**, 011303 (2023).
6. F. J. G. de Abajo, Optical excitations in electron microscopy. *Rev. Mod. Phys.* **82**, 209–275 (2010).
7. I. Kaminer, Y. T. Katan, H. Buljan, Y. Shen, O. Ilic, J. J. López, L. J. Wong, J. D. Joannopoulos, M. Soljačić, Efficient plasmonic emission by the quantum Čerenkov effect from hot carriers in graphene. *Nat. Commun.* **7**, ncomms11880 (2016).
8. V. Ginis, J. Danckaert, I. Veretennicoff, P., Tassin controlling Cherenkov radiation with transformation-optical metamaterials. *Phys. Rev. Lett.* **113**, 167402 (2014).
9. J. J. Aubert, U. Becker, P. J. Biggs, J. Burger, M. Chen, G. Everhart, P. Goldhagen, J. Leong, T. McCorriston, T. G. Rhoades, M. Rohde, S. C. C. Ting, S. L. Wu, Y. Y. Lee, Experimental observation of a heavy particle. *J. Phys. Rev. Lett.* **33**, 1404–1406 (1974).
10. W. Galbraith, J. V. Jelley, Light pulses from the night sky associated with cosmic rays. *Nature* **171**, 349–350 (1953).
11. X. Lin, H. Hu, S. Easo, Y. Yang, Y. Shen, K. Yin, M. P. Blago, I. Kaminer, B. Zhang, H. Chen, J. Joannopoulos, M. Soljačić, Y. Luo, A Brewster route to Cherenkov detectors. *Nat. Commun.* **12**, 5554 (2021).
12. O. Chamberlain, E. Segrè, C. Wiegand, T. Ypsilantis, Observation of antiprotons. *Phys. Rev. J. Archive* **100**, 947–950 (1955).
13. N. Rivera, I. Kaminer, Light-matter interactions with photonic quasiparticles. *Nat. Rev. Phys.* **2**, 538–561 (2020).
14. H. Hu, X. Lin, D. Liu, H. Chen, B. Zhang, Y. Luo, Broadband enhancement of Cherenkov radiation using dispersionless plasmons. *Adv. Sci.* **9**, 2200538 (2022).
15. S. Liu, P. Zhang, W. Liu, S. Gong, R. Zhong, Y. Zhang, M. Hu, Surface polariton Cherenkov light radiation source. *Phys. Rev. Lett.* **109**, 153902 (2012).
16. Z. Zhang, C. Du, J. Zhu, F. Li, B. Shen, X. Wang, P. Liu, Free-electron-driven frequency comb. *Laser Photon. Rev.* **17**, 202200886 (2023).
17. S. Huang, R. Duan, N. Pramanik, J. S. Herrin, C. Boothroyd, Z. Liu, L. J. Wong, Quantum recoil in free-electron interactions with atomic lattices. *Nat. Photonics* **17**, 224–230 (2023).
18. D. A. Alexander, A. Nomezine, L. A. Jarvis, D. J. Gladstone, B. W. Pogue, B. Bruza, Color Cherenkov imaging of clinical radiation therapy. *Light Sci. Appl.* **10**, 226 (2021).
19. T. M. Shaffer, E. C. Pratt, J. Grimm, Utilizing the power of Cerenkov light with nanotechnology. *Nat. Nanotechnol.* **12**, 106–117 (2017).
20. R. L. Hachadorian, P. Bruza, M. Jermyn, D. J. Gladstone, B. W. Pogue, L. A. Jarvis, Imaging radiation dose in breast radiotherapy by X-ray CT calibration of Cherenkov light. *Nat. Commun.* **11**, 2298 (2020).
21. X. Wang, L. Li, J. Li, P. Wang, J. Lang, Y. Yang, Cherenkov luminescence in tumor diagnosis and treatment: A review. *Photonics* **9**, 390 (2022).
22. N. Kotagiri, G. P. Sudlow, W. J. Akers, S. Achilefu, Breaking the depth dependency of phototherapy with Cerenkov radiation and low-radiance-responsive nanophotosensitizers. *Nat. Nanotechnol.* **10**, 370–379 (2015).
23. A. Kamkaew, L. Cheng, S. Goel, H. F. Valdovinos, T. E. Barnhart, Z. Liu, W. Cai, Cerenkov radiation induced photodynamic therapy using chlorin e6-loaded hollow mesoporous silica nanoparticles. *ACS Appl. Mater. Interfaces* **8**, 26630–26637 (2016).
24. H. Chen, M. Chen, Flipping photons backward: Reversed Cherenkov radiation. *Mater. Today* **14**, 34–41 (2011).
25. S. Xi, H. Chen, T. Jiang, L. Ran, J. Huangfu, B.-I. Wu, J. A. Kong, M. Chen, Experimental verification of reversed Cherenkov radiation in left-handed metamaterial. *Phys. Rev. Lett.* **103**, 194801 (2009).
26. S. Zhang, X. Zhang, Flipping a photonic shock wave. *Phys. Ther.* **2**, 91 (2009).
27. Y. Liu, X. Zhang, Metamaterials: A new frontier of science and technology. *Chem. Soc. Rev.* **40**, 2494–2507 (2011).
28. M. Kadic, G. W. Milton, M. Van Hecke, M. Wegener, 3D metamaterials. *Nat. Rev. Phys.* **1**, 198–210 (2019).
29. T. J. Cui, S. Zhang, A. Alù, M. Wegener, S. J. Pendry, J. Luo, Y. Lai, Z. Wang, X. Lin, H. Chen, P. Chen, R.-X. Wu, Y. Yin, P. Zhao, H. Chen, Y. Li, Z. Zhou, N. Engheta, V. Asadchy, C. Simovski, S. Tretyakov, B. Yang, S. D. Campbell, Y. Hao, D. H. Werner, S. Sun, L. Zhou, S. Xu, H.-B. Sun, Z. Zhou, Z. Li, G. Zheng, X. Chen, T. Li, S. Zhu, J. Zhou, J. Zhao, Z. Liu, Y. Zhang, Q. Zhang, M. Gu, S. Xiao, Y. Liu, X. Zhang, Y. Tang, G. Li, T. Zentgraf, K. Koshelev, Y. Kivshar, X. Li, T. Badloe, L. Huang, J. Rho, S. Wang, D. P. Tsai, A. Y. Bykov, A. V. Krasavin, A. V. Zayats, C. McDonnell, T. Ellenbogen, X. Luo, M. Pu, F. J. Garcia-Vidal, L. Liu, Z. Li, W. Tang, H. F. Ma, J. Zhang, Y. Luo, X. Zhang, H. C. Zhang, P. H. He, L. P. Zhang, X. Wan, H. Wu, S. Liu, W. X. Jiang, X. G. Zhang, C.-W. Qiu, Q. Ma, C. Liu, L. Li, J. Han, L. Li, M. Cotrufo, C. Caloz, Z.-L. Deck-Léger, A. Bahrami, O. Céspedes, E. Galiffi, P. A. Huidobro, Q. Cheng, J. Y. Dai, J. C. Ke, L. Zhang, V. Galdi, M. Di Renzo, Roadmap on electromagnetic metamaterials and metasurfaces. *J. Phys. Photonics* **6**, 032502 (2024).
30. Z. Zhang, L. Xu, T. Qu, M. Lei, Z.-K. Lin, X. Ouyang, J.-H. Jiang, J. Huang, Diffusion metamaterials. *Nat. Rev. Phys.* **5**, 218–235 (2023).
31. H. Hu, N. Chen, H. Teng, R. Yu, M. Xue, K. Chen, Y. Xiao, Y. Qu, D. Hu, J. Chen, Z. Sun, P. Li, F. J. G. de Abajo, Q. Dai, Gate-tunable negative refraction of mid-infrared polaritons. *Science* **379**, 558–561 (2023).
32. J. Fan, L. Zhang, S. Wei, Z. Zhang, S.-K. Choi, B. Song, Y. Shi, A review of additive manufacturing of metamaterials and developing trends. *Mater. Today* **50**, 303–328 (2021).
33. R. A. Shelby, D. R. Smith, S. Schultz, Experimental verification of a negative index of refraction. *Science* **292**, 77–79 (2001).
34. V. G. Veselago, The electrodynamics of substances with simultaneously negative values of ε and μ. *Sov. Phys. Usp.* **10**, 509–514 (1968).
35. D. V. Skryabin, Y. V. Kartashov, O. A. Egorov, M. Sich, J. K. Chana, L. E. Tapia Rodriguez, P. M. Walker, E. Clarke, B. Royall, M. S. Skolnick, D. N. Krizhanovskii, Backward Cherenkov radiation emitted by polariton solitons in a microcavity wire. *Nat. Commun.* **8**, 1554 (2017).
36. H. Hu, X. Lin, Y. Luo, Free-electron radiation engineering via structured environments. *Prog. Electromag. Res.* **171**, 75–88 (2021).

37. P. Genevet, D. Wintz, A. Ambrosio, A. She, R. Blanchard, F. Capasso, Controlled steering of Cherenkov surface plasmon wakes with a one-dimensional metamaterial. *Nat. Nanotechnol.* **10**, 804–809 (2015).
38. S. N. Galyamin, A. V. Tyukhtin, A. Kanareykin, P. Schoessow, Reversed Cherenkov-transition radiation by a charge crossing a left-handed medium boundary. *Phys. Rev. Lett.* **103**, 194802 (2009).
39. X. Shi, X. Lin, I. Kaminer, F. Gao, Z. Yang, J. D. Joannopoulos, M. Soljačić, B. Zhang, Superlight inverse Doppler effect. *Nat. Phys.* **14**, 1001–1005 (2018).
40. J. Chen, Y. Wang, B. Jia, T. Geng, X. Li, L. Feng, W. Qian, B. Liang, X. Zhang, M. Gu, S. Zhuang, Observation of the inverse Doppler effect in negative-index materials at optical frequencies. *Nat. Photonics* **5**, 239–242 (2011).
41. E. J. Reed, M. Soljačić, J. D. Joannopoulos, Reversed Doppler effect in photonic crystals. *Phys. Rev. Lett.* **91**, 133901 (2003).
42. C. Luo, M. Ibanescu, E. J. Reed, S. G. Johnson, J. D. Joannopoulos, Doppler radiation emitted by an oscillating dipole moving inside a photonic band-gap crystal. *Phys. Rev. Lett.* **96**, 043903 (2006).
43. N. Seddon, T. Bearpark, Observation of the inverse Doppler effect. *Science* **302**, 1537–1540 (2003).
44. X. Lin, B. Zhang, Normal Doppler frequency shift in negative refractive-index systems. *Laser Photon. Rev.* **13**, 1900081 (2019).
45. X. Lu, M. A. Shapiro, I. Mastovsky, R. J. Temkin, M. Conde, J. G. Power, J. Shao, E. E. Wisniewski, C. Jing, Generation of high-power, reversed-Cherenkov wake-field radiation in a metamaterial structure. *Phys. Rev. Lett.* **122**, 014801 (2019).
46. Z. Duan, X. Tang, Z. Wang, Y. Zhang, X. Chen, M. Chen, Y. Gong, Observation of the reversed Cherenkov radiation. *Nat. Commun.* **8**, 14901 (2017).
47. S. Antipov, L. Spentzouris, W. Gai, M. Conde, F. Franchini, R. Konecny, W. Liu, J. G. Power, Z. Yusof, C. Jing, Observation of wakefield generation in left-handed band of metamaterial-loaded waveguide. *J. Appl. Phys.* **104**, 014901 (2008).
48. S. N. Galyamin, A. V. Tyukhtin, Electromagnetic field of a charge traveling into an anisotropic medium. *Phys. Rev. E* **84**, 056608 (2011).
49. S. Xue, Y. Zeng, S. Zhu, H. Chen, Tunable Cherenkov radiation based on a van der Waals semiconductor α-MoO_3 and graphene hybrid. *Opt. Lett.* **47**, 2458–2461 (2022).
50. X. Guo, C. Wu, S. Zhang, D. Hu, S. Zhang, Q. Jiang, X. Dai, Y. Duan, X. Yang, Z. Sun, S. Zhang, H. Xu, Q. Dai, Mid-infrared analogue polaritonic reversed Cherenkov radiation in natural anisotropic crystals. *Nat. Commun.* **14**, 2532 (2023).
51. J. Tao, L. Wu, G. Zheng, S. Yu, Cherenkov polaritonic radiation in a natural hyperbolic material. *Carbon* **150**, 136–141 (2019).
52. Z. Gong, J. Chen, R. Chen, X. Zhu, C. Wang, X. Zhang, H. Hu, Y. Yang, B. Zhang, H. Chen, I. Kaminer, X. Lin, Interfacial Cherenkov radiation from ultralow-energy electrons. *Proc. Natl. Acad. Sci. U.S.A.* **120**, e2306601120 (2023).
53. C. Luo, M. Ibanescu, S. G. Johnson, J. D. Joannopoulos, Cerenkov radiation in photonic crystals. *Science* **299**, 368–371 (2003).
54. X. Lin, S. Easo, Y. Shen, H. Chen, B. Zhang, J. D. Joannopoulos, M. Soljačić, I. Kaminer, Controlling Cherenkov angles with resonance transition radiation. *Nat. Phys.* **14**, 816–821 (2018).
55. X. Gao, X. Zhao, R. Huang, S. Ma, X. Ma, T. Dong, Analysis and design of transition radiation in layered uniaxial crystals using tandem neural networks. *J. Opt. Soc. Am. B* **40**, 645–653 (2023).
56. Y. Yang, J.-W. Henke, A. S. Raja, F. J. Kappert, G. Huang, G. Arend, Z. Qiu, A. Feist, R. N. Wang, A. Tusnin, A. Tikan, C. Ropers, T. J. Kippenberg, Free-electron interaction with nonlinear optical states in microresonators. *Science* **383**, 168–173 (2024).
57. J. H. Gaida, H. Lourenço-Martins, M. Sivis, T. Rittmann, A. Feist, F. J. G. de Abajo, C. Ropers, Attosecond electron microscopy by free-electron homodyne detection. *Nat. Photon.* **18**, 509–515 (2024).
58. S. Huang, R. Duan, N. Pramanik, M. Go, C. Boothroyd, Z. Liu, L. J. Wong, Multicolor X-rays from free electron-driven van der Waals heterostructures. *Sci. Adv.* **9**, eadj8584 (2023).
59. M. Yannai, Y. Adiv, R. Dahan, K. Wang, A. Gorlach, N. Rivera, T. Fishman, M. Krüger, I. Kaminer, Lossless monochromator in an ultrafast electron microscope using near field THz radiation. *Phys. Rev. Lett.* **131**, 145002 (2023).
60. D. Zhang, Y. Zeng, Y. Bai, Z. Li, Y. Tian, R. Li, Coherent surface plasmon polariton amplification via free-electron pumping. *Nature* **611**, 55–60 (2022).
61. Y. Yang, A. Massuda, C. Roques-Carmes, S. E. Kooi, T. Christensen, S. G. Johnson, J. D. Joannopoulos, O. D. Miller, I. Kaminer, M. Soljačić, Maximal spontaneous photon emission and energy loss from free electrons. *Nat. Phys.* **14**, 894–899 (2018).
62. X.-Q. Yu, Y.-S. Zeng, L.-W. Song, D.-Y. Kong, S.-B. Hao, J.-Y. Gui, X.-J. Yang, Y. Xu, X.-J. Wu, Y.-X. Leng, Y. Tian, R.-X. Li, Megaelectronvolt electron acceleration driven by terahertz surface waves. *Nat. Photonics* **17**, 957–963 (2023).
63. L. J. Wong, I. Kaminer, O. Ilic, J. D. Joannopoulos, M. Soljačić, Towards graphene plasmon-based free-electron infrared to X-ray sources. *Nat. Photonics* **10**, 46–52 (2015).
64. C. Roques-Carmes, N. Rivera, A. Ghorashi, S. E. Kooi, Y. Yang, Z. Lin, J. Beroz, A. Massuda, J. Sloan, N. Romeo, Y. Yu, J. D. Joannopoulos, I. Kaminer, S. G. Johnson, M. Soljačić, A framework for scintillation in nanophotonics. *Science* **375**, eabm9293 (2022).
65. H. Hu, X. Lin, L. J. Wong, Q. Yang, D. Liu, B. Zhang, Y. Luo, Surface Dyakonov–Cherenkov radiation. *eLight* **2**, 2 (2022).
66. M. Shentcis, A. K. Budniak, X. Shi, R. Dahan, Y. Kurman, M. Kalina, H. Herzig Sheinfux, M. Blei, M. K. Svendsen, Y. Amouyal, S. Tongay, K. S. Thygesen, F. H. L. Koppens, E. Lifshitz, F. J. García de Abajo, L. J. Wong, I. Kaminer, Tunable free-electron X-ray radiation from van der Waals materials. *Nat. Photonics* **14**, 686–692 (2020).
67. X. Lin, H. Chen, Shaping free-electron radiation via van der Waals heterostructures. *Light Sci. Appl.* **12**, 187 (2023).
68. Z. Su, B. Xiong, Y. Xu, Z. Cai, J. Yin, R. Peng, Y. Liu, Manipulating Cherenkov radiation and Smith-Purcell radiation by artificial structures. *Adv. Opt. Mater.* **7**, 1801666 (2019).
69. Z. Su, F. Cheng, L. Li, Y. Liu, Complete control of Smith-Purcell radiation by graphene metasurfaces. *ACS Photonics* **6**, 1947–1954 (2019).
70. L. Jing, X. Lin, Z. Wang, I. Kaminer, H. Hu, E. Li, Y. Liu, M. Chen, B. Zhang, H. Chen, Polarization shaping of free-electron radiation by gradient bianisotropic metasurfaces. *Laser Photon. Rev.* **15**, 2000426 (2021).
71. I. de Leon, P. Berini, Amplification of long-range surface plasmons by a dipolar gain medium. *Nat. Photonics* **4**, 382–387 (2010).
72. M. C. Gather, K. Meerholz, N. Danz, K. Leosson, Net optical gain in a plasmonic waveguide embedded in a fluorescent polymer. *Nat. Photonics* **4**, 457–461 (2010).
73. A. Fang, T. Koschny, C. M. Soukoulis, Lasing in metamaterial nanostructures. *J Opt* **12**, 024013 (2010).
74. J. E. Geusic, H. M. Marcos, L. G. Van Uitert, Laser oscillations in Nd-doped yttrium aluminum, yttrium gallium and gadolinium garnets. *Appl. Phys. Lett.* **4**, 182–184 (1964).
75. F. Hide, M. A. Díaz-García, B. J. Schwartz, M. R. Andersson, Q. Pei, A. J. Heeger, Semiconducting polymers: A new class of solid-state laser materials. *Science* **273**, 1833–1836 (1996).
76. C. Qian, Y. Yang, Y. Hua, C. Wang, X. Lin, T. Cai, D. Ye, E. Li, I. Kaminer, H. Chen, Breaking the fundamental scattering limit with gain metasurfaces. *Nat. Commun.* **13**, 4383 (2022).
77. D. Ye, K. Chang, L. Ran, H. Xin, Microwave gain medium with negative refractive index. *Nat. Commun.* **5**, 5841 (2014).
78. W. Xu, W. J. Padilla, S. Sonkusale, Loss compensation in metamaterials through embedding of active transistor based negative differential resistance circuits. *Opt. Express* **20**, 22406–22411 (2012).
79. T. Jiang, K. Chang, L.-M. Si, L. Ran, H. Xin, Active microwave negative-index metamaterial transmission line with gain. *Phys. Rev. Lett.* **107**, 205503 (2011).
80. J. Olmos-Trigo, C. Sanz-Fernández, D. R. Abujetas, J. Lasa-Alonso, N. De Sousa, A. García-Etxarri, J. A. Sánchez-Gil, G. Molina-Terriza, J. J. Sáenz, Kerker conditions upon lossless, absorption, and optical gain regimes. *Phys. Rev. Lett.* **125**, 073205 (2020).
81. D. J. Bergman, M. I. Stockman, Surface plasmon amplification by stimulated emission of radiation: Quantum generation of coherent surface plasmons in nanosystems. *Phys. Rev. Lett.* **90**, 027402 (2003).
82. C. Wang, D. Zhang, J. Yue, H. Lin, X. Zhang, T. Zhang, C. Chen, T. Fei, On-chip optical sources of 3D photonic integration based on active fluorescent polymer waveguide microdisks for light display application. *PhotoniX* **4**, 13 (2023).
83. K. Yang, Y. Zhou, Y. Ling, K. Tsia, H. Zeng, K. Wong, Spectral period doubling and encoding of dissipative optical solitons via gain control. *PhotoniX* **5**, 26 (2024).
84. R. Chen, J. Chen, Z. Gong, X. Zhang, X. Zhu, Y. Yang, I. Kaminer, H. Chen, B. Zhang, X. Lin, Free-electron Brewster-transition radiation. *Sci. Adv.* **9**, eadh8098 (2023).
85. V. L. Ginzburg, Radiation of a uniformly moving electron due to its transition from one medium into another. *Sov. Phys. JETP* **16**, 15–28 (1946).
86. V. L. Ginzburg, V. N. Tsytovich, *Transition Radiation and Transition Scattering* (CRC Press, 1990).
87. X. Lin, I. Kaminer, X. Shi, F. Gao, Z. Yang, Z. Gao, H. Buljan, J. D. Joannopoulos, M. Soljačić, H. Chen, B. Zhang, Splashing transients of 2D plasmons launched by swift electrons. *Sci. Adv.* **3**, e1601192 (2017).
88. J. Chen, R. Chen, F. Tay, Z. Gong, H. Hu, Y. Yang, X. Zhang, C. Wang, I. Kaminer, H. Chen, B. Zhang, X. Lin, Low-velocity-favored transition radiation. *Phys. Rev. Lett.* **131**, 113002 (2023).
89. J. Chen, H. Chen, X. Lin, Photonic and plasmonic transition radiation from graphene. *J Opt* **23**, 034001 (2021).
90. Z. Gong, R. Chen, Z. Wang, X. Xi, Y. Yang, B. Zhang, H. Chen, I. Kaminer, X. Lin, Free-electron resonance transition radiation via Brewster randomness. *Proc. Natl. Acad. Sci. U.S.A.* **122**, e2413336122 (2025).
91. R. Chen, Z. Gong, J. Chen, X. Zhang, X. Zhu, H. Chen, X. Lin, Recent advances of transition radiation: Fundamentals and applications. *Mater. Today Electron.* **3**, 100025 (2023).
92. X. Xu, D. B. Cesar, S. Corde, V. Yakimenko, M. J. Hogan, C. Joshi, A. Marinelli, W. B. Mori, Generation of terawatt attosecond pulses from relativistic transition radiation. *Phys. Rev. Lett.* **126**, 094801 (2021).
93. G.-Q. Liao, Y.-T. Li, Y.-H. Zhang, H. Liu, X.-L. Ge, S. Yang, W.-Q. Wei, X.-H. Yuan, Y.-Q. Deng, B.-J. Zhu, Z. Zhang, W.-M. Wang, Z.-M. Sheng, L.-M. Chen, X. Lu, J.-L. Ma, X. Wang, J. Zhang, Demonstration of coherent terahertz transition radiation from relativistic laser-solid interactions. *Phys. Rev. Lett.* **116**, 205003 (2016).

94. K. D. de Vries, S. Prohira, Coherent transition radiation from the geomagnetically induced current in cosmic-ray air showers: Implications for the anomalous events observed by ANITA. *Phys. Rev. Lett.* **123**, 091102 (2019).
95. C. Wang, X. Chen, Z. Gong, R. Chen, H. Hu, H. Wang, Y. Yang, L. Tony, B. Zhang, H. Chen, X. Lin, Superscattering of light: Fundamentals and applications. *Rep. Prog. Phys.* **87**, 126401 (2024).
96. M. Voin, L. Schächter, Enhanced Cherenkov-wake amplification by an active medium. *Phys. Rev. Lett.* **112**, 054801 (2014).
97. G. Adamo, K. F. MacDonald, Y. H. Fu, C.-M. Wang, D. P. Tsai, F. J. García de Abajo, N. I. Zheludev, Light well: A tunable free-electron light source on a chip. *Phys. Rev. Lett.* **103**, 113901 (2009).
98. Z. Dang, Y. Huang, Z. Liu, L. Zheng, X. He, Z. Liu, Y. Dai, Z. Fang, Chiral Smith-Purcell radiation light source. *Adv. Opt. Mater.* **11**, 2300274 (2023).

Acknowledgments
Funding: X.L. acknowledges the partial support from Fundamental Research Funds for the Central Universities under grant no. 226-2024-00022, the National Natural Science Fund for Excellent Young Scientists Fund Program (Overseas) of China, the National Natural Science Foundation of China (NSFC) under grant no. 62475227, the National Natural Science Foundation of China (NSFC) under grant no. 62175212, and the Zhejiang Provincial Natural Science Fund Key Project under grant no. LZ23F050003. H.C. acknowledges the support from the Key Research and Development Program of the Ministry of Science and Technology under grant nos. 2022YFA1404704, 2022YFA1405200, and 2022YFA1404902; the Key Research and Development Program of Zhejiang Province under grant no. 2022C01036; and Fundamental Research Funds for the Central Universities. R.C. acknowledges the partial support from the National Natural Science Foundation of China (NSFC) under grant no. 623B2089. B.Z. acknowledges the support from Singapore National Research Foundation Competitive Research Program No. NRF-CRP23-2019-0007. Y.Y. acknowledges the support from the National Natural Science Foundation of China Excellent Young Scientists Fund (HKU 12222417), Hong Kong Research Grant Council Strategic Topics grant no. STG3/E-704/23-N, the startup fund of The University of Hong Kong, and Asian Young Scientist Fellowship. **Author contributions:** Conceptualization: R.C. and X.L. Investigation: R.C. Visualization: R.C., Z.G., Z.W., X.X., Bowen Zhang, Y.Y., Baile Zhang, H.C., I.K., and X.L. Supervision: X.L., Baile Zhang., H.C., and I.K. Writing—original draft: R.C. and X.L. Writing—review and editing: Z.G., Z.W., X.X., Bowen Zhang, Y.Y., Baile Zhang, H.C., and I.K. **Competing interests:** The authors declare that they have no competing interests. **Data and materials availability:** All data needed to evaluate the conclusions in the paper are present in the paper and/or the Supplementary Materials.

Submitted 16 August 2024
Accepted 28 February 2025
Published 4 April 2025
10.1126/sciadv.ads5113